Transactions on Computer Science and Intelligent Systems Research
ISSN: 2960-1800, eISSN: 2960-2238 | Volume 13
AMMSAC 2026

Comparing Surface and Canopy Urban Heat Islands in Hong Kong with Population Heat Exposure: Integrating Satellite LST and Ground Weather Observations

Yelin Luo [1, *]

[1] Guanghua Cambridge International School, Shanghai 200000, China

* Corresponding Author Email: lylyly080916@163.com

Abstract. Satellite land surface temperature (LST) is widely used to map urban heat, yet it characterizes the radiative state of surfaces rather than the near-surface air that people experience. This study quantitatively compares the surface urban heat island (SUHI) and the canopy-layer (air-temperature) urban heat island (CUHI) over Hong Kong, a high-density coastal subtropical city, and evaluates their implications for population heat exposure. SUHI is derived from Moderate Resolution Imaging Spectroradiometer (MODIS) day/night LST (1 km) and Landsat Collection-2 surface temperature (100 m) for the 2023–2024 warm season, after water masking and an elevation-corrected non-built reference; CUHI is derived from 25 Hong Kong Observatory (HKO) automatic weather stations. Population heat exposure is then modeled with WorldPop 100 m population under two metrics: a surface-temperature proxy and a station-interpolated air-temperature field (leave-one-out mean absolute error 0.3–0.4 °C). Three findings emerge. (1) The surface heat island is much larger in magnitude than the canopy heat island (SUHI spatial range 6–14 °C versus CUHI ~2 °C). (2) Their spatial coupling is weak and scale-dependent: at 1 km no statistically robust station-level association is found (day and night bootstrap confidence intervals include zero), and only a moderate daytime rank association emerges at 100 m (Spearman $\rho=0.53$, $p=0.01$). (3) The two exposure metrics diverge: a relative surface proxy ranks 79% of residents in upper-quartile surface heat, whereas the air-temperature metric—tied to local heat-health thresholds—identifies 10% of residents (7% of the elderly) exposed to very-hot-day air temperatures (≥33 °C). Overall, LST usefully maps the surface thermal environment but cannot, without calibration, substitute for canopy-level heat exposure in a high-density coastal city.

Keywords: surface urban heat island; canopy urban heat island; land surface temperature; air temperature; population heat exposure; MODIS; Hong Kong; spatial interpolation; statistical modeling.

1. Introduction

The urban heat island (UHI) is observed through two distinct lenses. Thermal remote sensors measure the surface UHI (SUHI) from upwelling radiance, whereas screen-height weather stations measure the canopy-layer or air-temperature UHI (CUHI), which is the heat actually inhaled by residents [1,2]. The two share energy-balance drivers but differ in source area, diurnal timing, and sensitivity to vegetation, roughness, advection, and at0mospheric stability, so one should not be treated as a direct proxy for the other [1, 3]. A recent global analysis shows that surface and canopy UHIs even diverge in their long-term trends and drivers, the daytime surface UHI trend being several times the canopy UHI trend [3].

This distinction matters most where satellite land surface temperature (LST) is used to infer human heat exposure. Hong Kong is an instructive case: a compact high-rise coastal subtropical territory whose UHI is predominantly nocturnal and can reverse to a daytime urban "cool island," shaped by sea-land breezes, steep terrain and dense urban canyons [4, 5]. Hong Kong is unusual among Chinese cities in publishing a dense network of open, quality-controlled station air temperatures, which makes a like-for-like SUHI-CUHI comparison feasible. Heat is a public-health concern here: mortality risk rises disproportionately in high-UHI districts and among the elderly [6, 7, 8].

Prior Hong Kong work has separately quantified the air-temperature UHI [4, 9], the satellite SUHI in the Greater Bay Area [10], and, very recently, the diurnal air-surface temperature relationship across land-use and local-climate zones [11]. What remains underexplored is a single, consistent comparison of SUHI and CUHI that is carried through to population heat exposure under both surface and air-temperature metrics. This study provides such a focused assessment, with three objectives: (i) to quantify day and night SUHI and CUHI on a common Hong Kong frame; (ii) to test their spatial coupling and its scale dependence; and (iii) to compare population (and elderly) heat exposure modeled from a surface proxy versus an interpolated air-temperature field.

2. Study Area and Data

Hong Kong (~1,100 km², ~7.4 million residents) is a subtropical coastal territory of dense high-rise development interspersed with steep country parks rising to 957 m. The analysis uses the 2023 and 2024 warm seasons (June-September). Data sources are summarized in Table 1. SUHI is derived from Moderate Resolution Imaging Spectroradiometer (MODIS) MOD11A2 (1 km, 8-day day/night LST) [12] and Landsat 8/9 Collection-2 Level-2 surface temperature (100 m, 13 clear scenes). CUHI uses daily mean/maximum/minimum air temperature from 25 Hong Kong Observatory (HKO) automatic weather stations spanning urban, new-town, rural and high-elevation settings. Population exposure uses WorldPop 2020 100 m counts and age structure (65+) [13]. European Space Agency (ESA) WorldCover (10 m) provides water and built-up fractions, and the Copernicus GLO-30 digital elevation model (DEM) provides elevation; all gridded products were accessed without restricted credentials. The station network is shown in Fig. 1.

Table 1. Data sources used in this study.

Dataset	Variable	Resolution	Period	Access
MODIS MOD11A2 v061	LST day & night	1 km, 8-day	2023–24 summer	Planetary Computer
Landsat 8/9 C2 L2	Surface temperature	100 m	2023–24 summer	Planetary Computer
HKO weather stations	Air temp (mean/max/min)	25 stations	2023–24 summer	data.gov.hk
WorldPop	Population + age (65+)	100 m	2020	worldpop.org
ESA WorldCover v200	Land cover (water/built)	10 m	2021	Planetary Computer
Copernicus DEM GLO-30	Elevation	30 m	-	Planetary Computer

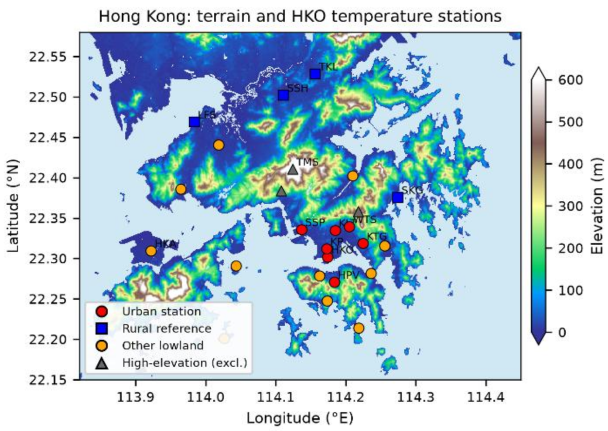

Figure 1. Hong Kong terrain (Copernicus DEM) and the 25 HKO temperature stations, classified as urban, rural-reference, other-lowland, and high-elevation (excluded from intensity statistics).

3. Methods

3.1. Periods and Day/Night Definitions

Warm-season (June-September) 2023–2024 LST is composited separately for day and night. Daytime surface heat is paired with station daily maximum air temperature (Tmax) and nighttime with daily minimum (Tmin), avoiding the need for sub-daily station archives.

3.2. Surface Heat Island

LST was scaled to °C, quality-screened (Landsat QA_PIXEL cloud/shadow bits; MODIS valid-range), and water-masked using ESA WorldCover (pixels with >20% water removed to suppress nighttime sea contamination in this coastal setting). SUHI intensity is the LST anomaly relative to a reference defined as non-built (built-up fraction <5%), low-elevation (<100 m) and non-water pixels. Rural-station-pixel references were retained only as a sensitivity test. Both MODIS 1 km (day and night) and Landsat 100 m (day) are reported to expose scale effects.

3.3. Canopy Heat Island

Station air temperatures were elevation-corrected to sea level using an environmental lapse rate of 6.5 °C/km, isolating the urban signal from topography; the three high-elevation stations (>100 m) were excluded from intensity statistics. Following the canonical Hong Kong scheme, urban references (HKO Headquarters, King's Park) were contrasted with rural references (Ta Kwu Ling, Tsak Yue Wu), complemented by a broader lowland urban/rural grouping [9].

3.4. SUHI-CUHI Comparison

The surface and canopy heat-island intensities are defined, relative to a common non-urban reference, as

$$\Delta T_s = T_{s,u} - T_{s,r} \quad , \qquad \Delta T_a = T_{a,u} - T_{a,r} \tag{1}$$

where Ts is land surface temperature and Ta is screen-height air temperature, and subscripts u and r denote the urban and non-urban reference domains. At each lowland station the co-located SUHI anomaly was sampled and paired with the station CUHI anomaly. Because the network is small (n=13–22), the relationship is treated as exploratory: Pearson r, Spearman ρ, two-sided p, and bootstrap 95% confidence intervals (CIs) are reported. Magnitudes are summarized by robust percentile ranges (p5-p95) rather than extrema.

3.5. Population Heat Exposure Modeling

Two metrics are computed, following population-weighted exposure approaches [14]. (a) Surface proxy: a population-weighted LST and the share of residents in upper-quartile surface heat, using relative thresholds because LST has no absolute physiological meaning. (b) Air temperature: lowland, elevation-corrected station Tmax and Tmin were interpolated (inverse-distance weighting; nearest-station as sensitivity) to a 100 m field and validated by leave-one-out cross-validation (LOO). Local heat-health thresholds were then applied—very-hot-day Tmax ≥ 33 °C and hot-night Tmin ≥ 28 °C—to compute exposed population and elderly. The two metrics are also compared in terms of where they place the upper-quartile heat burden. If interpolation skill were poor, the air metric would be reported only as a coarse sensitivity analysis; in practice LOO skill was high.

For either field, the population-weighted mean temperature is

$$T_{pw} = (\Sigma p_i\, T_i) / (\Sigma p_i) \tag{2}$$

where pi and Ti are the population count and temperature of grid cell i; the share of residents above a heat threshold is computed analogously by summing population over cells exceeding the threshold.

4. Results

4.1. Surface Heat Island

The warm-season SUHI is strongest by day and weaker at night (Fig. 2), consistent with the daytime-dominant surface heat island reported across global cities [15]. After water masking and referencing, the daytime surface anomaly spans 6.2 °C (p5-p95) at 1 km and 14.4 °C at 100 m, against a much smaller 3.0 °C at night (1 km). The finer Landsat field reveals intra-urban contrasts that the 1 km product smooths away, including very hot reclaimed/transport surfaces (e.g., the airport) and a comparatively moderate dense urban core—consistent with the daytime urban-canyon shading characteristic of high-rise Hong Kong.

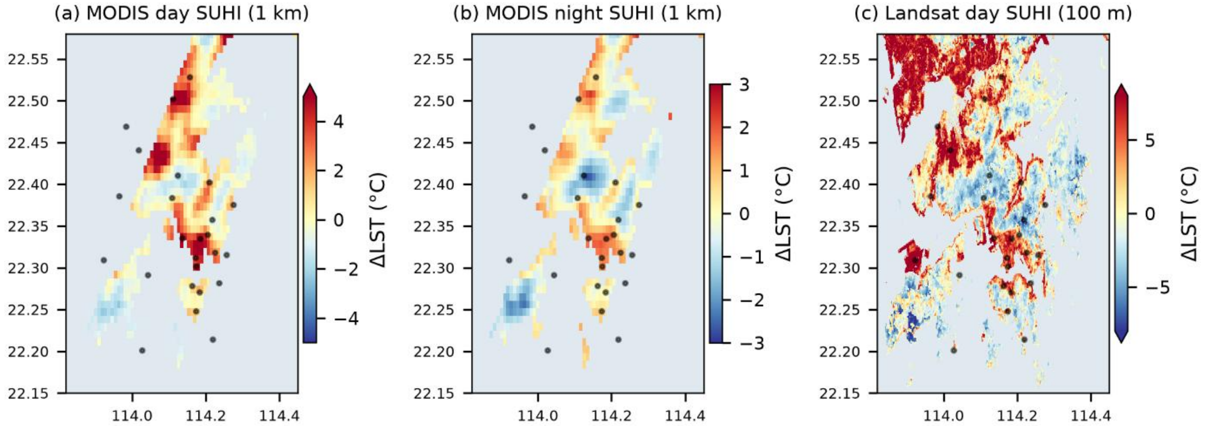

Figure 2. Warm-season surface urban heat island after water masking: (a) MODIS daytime (1 km), (b) MODIS night-time (1 km), and (c) Landsat daytime (100 m). Values are LST anomalies relative to a non-built low-elevation reference.

4.2. SUHI-CUHI Divergence and Scale Dependence

The canopy heat island is an order of magnitude smaller than the surface signal: the elevation-corrected CUHI spans ~2.6 °C (day) and ~1.9 °C (night) across lowland stations, with a daytime urban cool island (urban-rural Tmax -0.46 °C) and a nighttime warm island (+0.80 °C), in agreement with Hong Kong's known nocturnal UHI regime [4, 5]. Crucially, the spatial coupling between surface and air anomalies is weak and scale-dependent (Fig. 3): at 1 km neither the daytime (r=0.43, p=0.14) nor the nighttime (r=0.26, p=0.40) association is statistically robust, with bootstrap CIs including zero; only at 100 m does a moderate daytime rank association emerge (Spearman ρ=0.53, p=0.01, n=22). The much larger surface magnitude, together with this weak and scale-dependent coupling, echoes the surface-canopy divergence reported globally [3], while cautioning that the agreement is partial and resolution-sensitive. Intensity and correlation statistics are summarized in Table 2.

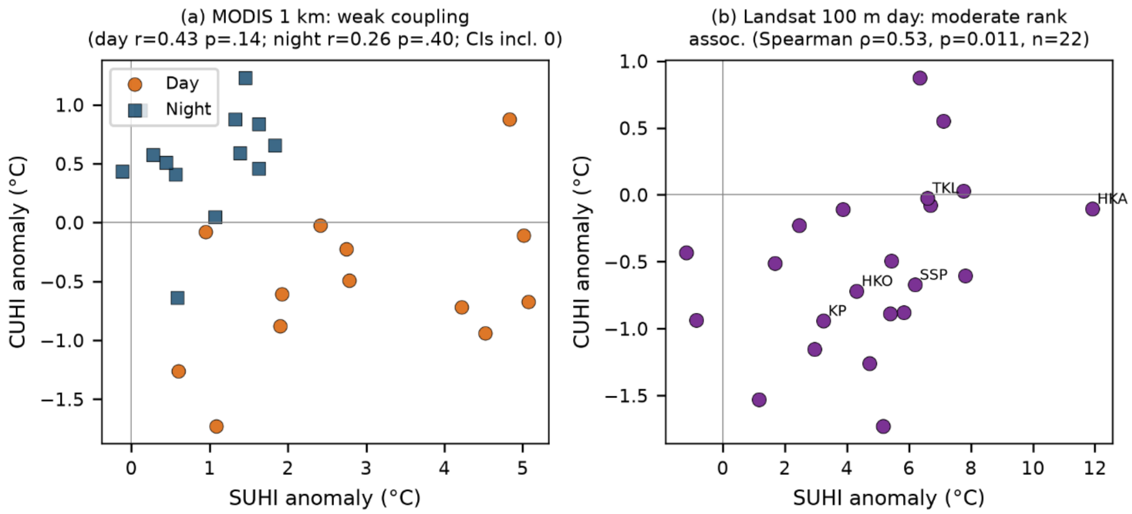

Figure 3. Station-level SUHI-CUHI relationship: (a) at MODIS 1 km, day and night couplings are weak (bootstrap CIs include zero); (b) at Landsat 100 m, a moderate daytime rank association emerges (Spearman ρ=0.53, p=0.01).

Table 2. Summary of SUHI and CUHI intensities and their exploratory spatial association (lowland stations).

Quantity	Day	Night
SUHI amplitude, MODIS 1 km (p5-p95)	6.2 °C	3.0 °C
SUHI amplitude, Landsat 100 m (p5-p95)	14.4 °C	-
CUHI amplitude (lowland stations)	2.6 °C	1.9 °C
CUHI urban-rural (elevation-corrected)	-0.46 °C	+0.80 °C
SUHI-CUHI MODIS 1 km: Pearson r (p)	0.43 (0.14)	0.26 (0.40)
SUHI-CUHI Landsat 100 m: Spearman ρ (p)	0.53 (0.01)	-
Pop. very-hot-day air Tmax≥33 °C	10% (7% elderly)	-
Pop. upper-quartile surface heat	79% (79% elderly)	-

4.3. Population Heat Exposure under Two Metrics

The two exposure metrics give markedly different pictures of the same population (Fig. 4). The surface proxy is high everywhere people live—population-weighted daytime LST is 39.2 °C versus an area mean of 35.1 °C, and 79% of residents (and 79% of the elderly) fall in the upper surface-heat quartile—but it can only rank relative hazard. The station-interpolated air-temperature field, which is reliable (LOO mean absolute error (MAE) 0.44 °C for Tmax, 0.28 °C for Tmin), ties exposure to absolute heat-health thresholds: population-weighted Tmax is 32.2 °C and 10% of residents (7% of the elderly) experience very-hot-day air temperatures (≥33 °C), concentrated in the inland urban basins of Kowloon and the northwestern new towns. Thus the choice of metric, not just the data source, reshapes who is counted as heat-exposed.

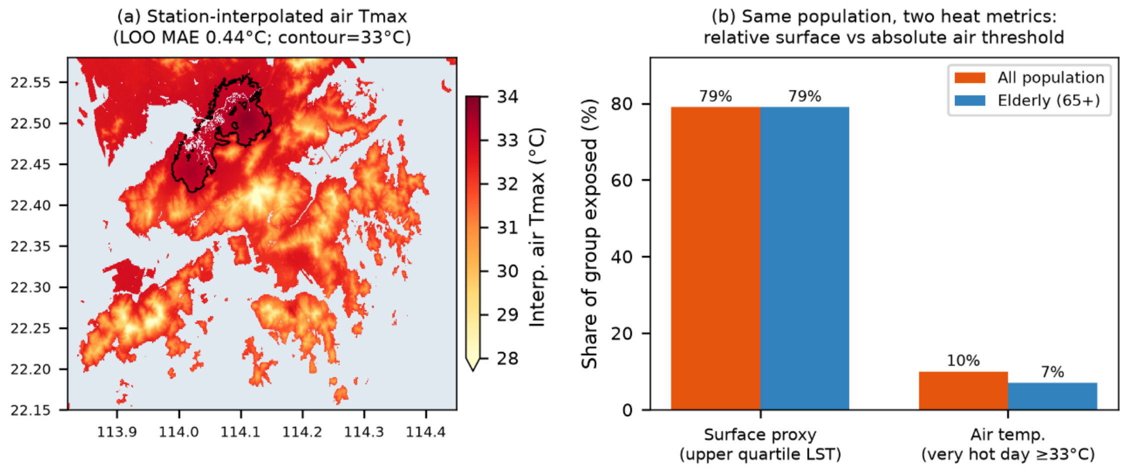

Figure 4. Population heat exposure under two metrics: (a) station-interpolated air Tmax (LOO MAE 0.44 °C) with the 33 °C very-hot-day contour; (b) share of all residents and of the elderly flagged as exposed by a relative surface-temperature proxy versus an absolute air-temperature threshold.

5. Discussion

The results support a single, practical message: in a high-density coastal city, satellite LST and station air temperature are not interchangeable for heat-exposure assessment. They differ in magnitude by roughly an order of magnitude, couple only weakly and in a scale-dependent way, and—because LST lacks an absolute physiological threshold—yield very different exposure counts. A surface-only assessment would flag four-fifths of the population as "hot," whereas the air-temperature metric isolates the ~10% facing genuinely extreme daytime air temperatures, the group most relevant to the elevated heat-mortality risk documented for high-UHI Hong Kong districts and older residents [6, 7]. Methodologically, this argues for using LST to characterize the surface thermal environment and to prioritize where to densify observations, but for calibrating to, or interpolating, air temperature before drawing human-exposure conclusions—extending recent Hong Kong air-surface analyses [11] toward population outcomes.

Several limitations should be read alongside these findings. The 1 km MODIS product is coarse for an intricate coastline and, even after masking, residual mixed pixels temper the nighttime analysis; the station network (n=25) limits statistical power, so the SUHI-CUHI associations are exploratory rather than confirmatory; the air-temperature field is interpolated from sparse points (albeit with low LOO error) rather than physically modelled; population is fixed at 2020 while LST spans 2023–2024; and the analysis covers two warm seasons, so no long-term trend is claimed. Promising extensions include an LST-to-air-temperature fusion model with land-cover and morphology covariates, local-climate-zone stratification, and higher-resolution night-time thermal data.

6. Conclusion

Across Hong Kong, the surface and canopy urban heat islands diverge in magnitude, couple only weakly and scale-dependently, and translate into different population heat-exposure pictures. Land surface temperature reliably maps the surface thermal environment, but it cannot, without calibration to air temperature, represent the heat exposure that residents actually experience. For high-density coastal cities, integrating satellite LST with ground station observations is therefore a prerequisite, not an enhancement, for credible population heat-exposure modeling.

References

[1] J.A. Voogt, T.R. Oke, Thermal remote sensing of urban climates, Remote Sens. Environ. 86 (2003) 370-384.

[2] T.R. Oke, The energetic basis of the urban heat island, Q. J. R. Meteorol. Soc. 108 (1982) 1-24.

[3] H. Du, W. Zhan, J. Voogt, B. Bechtel, T.C. Chakraborty, Z. Liu, et al., Contrasting trends and drivers of global surface and canopy urban heat islands, Geophys. Res. Lett. 50 (2023) e2023GL104661.

[4] W. Wang, B. Chen, Y. Xu, W. Zhou, X. Wang, Urban heat islands in Hong Kong: bonding with atmospheric stability, Atmos. Sci. Lett. 22 (2021) e1032.

[5] C. Ren, K. Wang, Y. Shi, Y.T. Kwok, T.E. Morakinyo, T.-C. Lee, et al., Investigating the urban heat and cool island effects during extreme heat events in high-density cities: a case study of Hong Kong from 2000 to 2018, Int. J. Climatol. 41 (2021) 6736-6754.

[6] J.Y. Ho, Y. Shi, K.K.L. Lau, E.Y.Y. Ng, C. Ren, W.B. Goggins, Urban heat island effect-related mortality under extreme heat and non-extreme heat scenarios: a 2010-2019 case study in Hong Kong, Sci. Total Environ. 858 (2023) 159791.

[7] J. Hua, X. Zhang, C. Ren, Y. Shi, T.-C. Lee, Spatiotemporal assessment of extreme heat risk for high-density cities: a case study of Hong Kong from 2006 to 2016, Sustain. Cities Soc. 64 (2021) 102507.

[8] W.B. Goggins, E.Y.Y. Chan, E. Ng, C. Ren, L. Chen, Effect modification of the association between short-term meteorological factors and mortality by urban heat islands in Hong Kong, PLoS ONE 7 (2012) e38551.

[9] L.W. Siu, M.A. Hart, Quantifying urban heat island intensity in Hong Kong SAR, China, Environ. Monit. Assess. 185 (2013) 4383-4398.

[10] X. Xu, Y. Wu, G. Lin, J. Gong, K. Chen, Exploring diurnal and seasonal variabilities in surface urban heat island intensity in the Guangdong-Hong Kong-Macao Greater Bay Area, J. Geogr. Sci. 34 (2024) 1472-1492.

[11] I.A. Adeniran, M. Nazeer, M.S. Wong, J. Yang, P.-W. Chan, Diurnal air-surface temperature dynamics in Hong Kong: an analysis across land use and climate zones, Int. J. Climatol. 46 (2026) e70297.

[12] Z. Wan, New refinements and validation of the collection-6 MODIS land-surface temperature/emissivity product, Remote Sens. Environ. 140 (2014) 36-45.

[13] A.J. Tatem, WorldPop, open data for spatial demography, Sci. Data 4 (2017) 170004.

[14] C. Tuholske, K. Caylor, C. Funk, A. Verdin, S. Sweeney, K. Grace, et al., Global urban population exposure to extreme heat, Proc. Natl. Acad. Sci. U.S.A. 118 (2021) e2024792118.

[15] S. Peng, S. Piao, P. Ciais, P. Friedlingstein, C. Ottle, F.-M. Bréon, et al., Surface urban heat island across 419 global big cities, Environ. Sci. Technol. 46 (2012) 696-703.